

PDF hosted at the Radboud Repository of the Radboud University Nijmegen

The following full text is a publisher's version.

For additional information about this publication click this link.

<http://hdl.handle.net/2066/137475>

Please be advised that this information was generated on 2021-09-28 and may be subject to change.

Mosquito and *Drosophila* entomobirnaviruses suppress dsRNA- and siRNA-induced RNAi

Koen W.R. van Cleef^{1,†}, Joël T. van Mierlo^{1,†}, Pascal Miesen¹, Gijs J. Overheul¹, Jelke J. Fros², Susan Schuster¹, Marco Marklewitz³, Gorben P. Pijlman², Sandra Junglen³ and Ronald P. van Rij^{1,*}

¹Department of Medical Microbiology, Radboud University Nijmegen Medical Centre, Radboud Institute for Molecular Life Sciences, P.O. Box 9101, 6500 HB Nijmegen, The Netherlands, ²Laboratory of Virology, Wageningen University, Droevendaalsesteeg 1, 6708 PB Wageningen, The Netherlands and ³Institute of Virology, University of Bonn Medical Centre, Sigmund Freud Str. 25, 53127 Bonn, Germany

Received July 8, 2013; Revised May 27, 2014; Accepted May 28, 2014

ABSTRACT

RNA interference (RNAi) is a crucial antiviral defense mechanism in insects, including the major mosquito species that transmit important human viruses. To counteract the potent antiviral RNAi pathway, insect viruses encode RNAi suppressors. However, whether mosquito-specific viruses suppress RNAi remains unclear. We therefore set out to study RNAi suppression by *Culex* Y virus (CYV), a mosquito-specific virus of the *Birnaviridae* family that was recently isolated from *Culex pipiens* mosquitoes. We found that the *Culex* RNAi machinery processes CYV double-stranded RNA (dsRNA) into viral small interfering RNAs (vsiRNAs). Furthermore, we show that RNAi is suppressed in CYV-infected cells and that the viral VP3 protein is responsible for RNAi antagonism. We demonstrate that VP3 can functionally replace B2, the well-characterized RNAi suppressor of Flock House virus. VP3 was found to bind long dsRNA as well as siRNAs and interfered with Dicer-2-mediated cleavage of long dsRNA into siRNAs. Slicing of target RNAs by pre-assembled RNA-induced silencing complexes was not affected by VP3. Finally, we show that the RNAi-suppressive activity of VP3 is conserved in *Drosophila* X virus, a birnavirus that persistently infects *Drosophila* cell cultures. Together, our data indicate that mosquito-specific viruses may encode RNAi antagonists to suppress antiviral RNAi.

INTRODUCTION

RNA interference (RNAi) is a cellular mechanism that regulates gene expression in a broad range of eukaryotes. In

plants (1), insects (2–4), nematodes (5,6), and fungi (7), the RNAi pathway is a crucial antiviral defense mechanism (reviewed in (8,9)). The antiviral potential of RNAi in vertebrates has only recently been demonstrated (10,11). For insects, the antiviral RNAi pathway is most extensively studied in *Drosophila melanogaster*. The current model for antiviral RNAi in *Drosophila* is that virus-derived double-stranded RNA (dsRNA) is processed by Dicer-2 (Dcr-2) into viral small interfering RNA (vsiRNA) duplexes that associate with Argonaute-2 (AGO2) within the RNA-induced silencing complex (RISC) (9). One strand of the vsiRNA duplex is retained in RISC to guide the identification and AGO2-mediated cleavage (slicing) of complementary viral RNAs (9). The detection of vsiRNAs during infections of *Drosophila* cell lines and adult flies supports this model (12,13). Moreover, the hypersensitivity of *Drosophila* RNAi pathway mutants to virus infections confirms the important role of RNAi in antiviral defense (2–4,14–19).

Insect viruses encode viral suppressors of RNAi (VSRs) to counteract the antiviral RNAi pathway. For example, the Flock House virus (FHV) B2 and *Drosophila* C virus (DCV) 1A proteins bind and shield long dsRNA from Dcr-2 cleavage (2,5,20,21). FHV B2 additionally binds siRNA duplexes, which inhibits their loading into RISC (5,20). The 1A protein of Cricket paralysis virus (CrPV) and viral protein 1 (VP1) of Nora virus were recently shown to inhibit AGO2 Slicer activity (22,23). In general, RNAi suppressor proteins of different virus families that target the same step in the RNAi pathway do not share sequence identity or structural conservation. Thus, insect viruses independently evolved a diverse set of RNAi antagonists that suppress the antiviral RNAi pathway by distinct mechanisms.

Mosquitoes are vectors for the transmission of arthropod-borne (arbo) viruses that can cause serious disease in humans, such as Dengue virus (DENV), West Nile virus (WNV) and Chikungunya virus (24). In addition,

*To whom correspondence should be addressed. Tel: +31 24 3617574; Email: r.vanrij@ncmls.ru.nl

†The authors wish it to be known that, in their opinion, the first two authors should be regarded as Joint First Authors.

mosquitoes are hosts to a diverse array of mosquito-specific viruses that are not transmitted to vertebrates (25–29). These viruses do not cause human disease, but they are of interest with regard to human health. Mosquito-specific viruses infect mosquito species that act as important vectors for human arbovirus transmission. Activation and suppression of antiviral immune pathways by mosquito-specific viruses may affect the ability of a vector mosquito to transmit co-infecting arboviruses. Currently, however, not much is known about the interactions between the mosquito's immune system and the different classes of mosquito viruses.

As is observed in virus infections of *Drosophila*, vsiRNAs are detected in mosquitoes and mosquito cell lines infected with arboviruses and mosquito-specific viruses (12,13). In addition, knockdown of RNAi pathway components in mosquitoes results in higher virus titers after infection with different arboviruses (30–32). These results show that, also in mosquitoes, the RNAi pathway serves as an important antiviral defense mechanism. Despite the antiviral activity of the mosquito RNAi pathway against a broad range of viruses, reports on VSR activity in viruses that infect mosquitoes are limited. VSRS have thus far only been identified in a few arboviruses from the genera *Alphanodavirus* (*Nodaviridae* family) and *Flavivirus* (*Flaviviridae* family) (21,33–35). Whether mosquito-specific viruses suppress RNAi is unknown.

Nodamura virus (NoV), like FHV a member of the *Alphanodavirus* genus, was first isolated from *Culex tritaeniorhynchus* mosquitoes in Japan (36). Successful experimental infections in vertebrates, and the detection of neutralizing antibodies in pigs, suggest that NoV is a mosquito-transmitted arbovirus (37). The B2 protein of NoV, like FHV B2, inhibits RNAi by binding long dsRNA as well as siRNA duplexes (21,33). More recently, the non-coding subgenomic flavivirus RNAs (sfRNAs) of WNV and DENV, two arboviruses from the *Flavivirus* genus, were shown to suppress RNAi (34). sfRNAs are abundantly produced during flavivirus infection and result from incomplete degradation of the genomic RNA (38). Probably because of their stem-loop structure, sfRNA molecules compete with Dicer substrates, thereby decreasing Dicer activity. DENV non-structural protein 4B (NS4B) was suggested to inhibit Dicer function through an undefined mechanism (35).

The identification and characterization of viral immune antagonists may provide important insights into the mechanisms, components and regulators of immune pathways. For example, the observation that two unrelated RNA viruses encode Slicer antagonists indicates that slicing of viral target RNAs is an important aspect of the antiviral RNAi response (22,23). To begin to understand the diversity of RNAi-suppressive activities in mosquito viruses, we set out to study RNAi suppression by the mosquito-specific *Culex Y* virus (CYV). CYV is a bisegmented dsRNA virus from the *Entomobirnavirus* genus within the *Birnaviridae* family that was recently isolated from *Culex pipiens* mosquitoes in Germany (27). Isolation of the highly related Espirito Santo virus and Mosquito X virus in Brazil and China, respectively, indicates that these entomobirnaviruses are widely distributed in nature (28,29).

Here, we demonstrate that CYV is a target of the *Culex* RNAi machinery. Furthermore, we show that CYV and *Drosophila X* virus (DXV), like CYV a member of the *Entomobirnavirus* genus, suppress the RNAi pathway during infection. The entomobirnavirus RNAi suppressor activity was mapped to VP3 and we show that the VP3 proteins can rescue the replication of a B2-deficient FHV RNA1 replicon. Finally, we demonstrate that the VP3 proteins bind long dsRNA as well as siRNAs and that they inhibit the production of siRNAs by Dcr-2. To our knowledge, we describe the first VSR of a mosquito-specific virus.

MATERIALS AND METHODS

Cells and viruses

Drosophila melanogaster S2, *Culex quinquefasciatus* Hsu and *Culex tarsalis* CT cells were cultured in Schneider's *Drosophila* medium (Life Technologies) at 25°C (S2 cells) or 28°C (Hsu and CT cells). The medium was supplemented with 10% heat-inactivated fetal bovine serum (FBS; PAA Laboratories), 50 U/ml penicillin and 50 µg/ml streptomycin (pen/strep; Life Technologies). *Aedes albopictus* U4.4 cells were maintained at 28°C in Leibovitz's L-15 medium (Life Technologies) supplemented with 10% heat-inactivated FBS, 2% tryptone phosphate broth (Sigma-Aldrich), 1× MEM non-essential amino acids (Life Technologies) and pen/strep. CYV and DXV were propagated in S2 cells.

Plasmids, radioactively-labeled probes, recombinant proteins and western blot analysis

The cloning and origin of plasmids, the production of radioactively-labeled probes, the purification of recombinant proteins and western blot analysis are described in the Supplementary Data.

Massive parallel sequencing of small RNAs

RNA was isolated from CYV-infected CT cells at 3 days post-infection using Isol-RNA Lysis Reagent (5 PRIME) and 30 µg of the RNA was separated on a 15% polyacrylamide/7M urea/0.5× TBE gel. The 19- to 33-nt small RNA fraction was cut from gel using ³²P end-labeled RNA oligos as size markers. The RNA was eluted in 0.3 M of NaOAc, precipitated in 100% EtOH and dissolved in 10 µl of H₂O. The small RNA library was prepared with the TruSeq Small RNA Sample Preparation Kit (Illumina) according to the manufacturer's instructions. After amplification, the library was separated on a 6% polyacrylamide/1× TBE gel. The PCR product corresponding to the amplified small RNAs was cut from gel, eluted in 0.3 M of NaOAc, precipitated in 100% EtOH in the presence of 20 µg of glycogen and reconstituted in 10 µl of 10 mM Tris-HCl. The library was sequenced on an Illumina HiSeq 2500 by Baseclear (www.baseclear.nl). FASTQ sequence reads were generated with the Illumina Casava pipeline (version 1.8.3) and initial quality assessment was performed by Baseclear using in-house scripts and the FASTQC quality control tool (version 0.10.0). FASTQ sequence reads that passed this quality

control were deposited in the Sequence Read Archive (SRA) under accession number SRP041409.

The sequence data were analyzed with Galaxy (39). Sequence reads were clipped from the adapter sequence (TruSeq 3' adapter index #8) and mapped with Bowtie (version 1.1.2) (40) to the CYV reference genome (GenBank accession numbers: JQ659254 and JQ659255 for genome segments A and B, respectively). A size profile of the viral small RNAs was obtained from all reads that mapped to the CYV genome with a maximum of one mismatch. The 5' ends of the 21-nt CYV-mapping reads were plotted onto the viral genome to analyze the genome distribution of the vsRNAs.

RNAi reporter assays

RNAi reporter assays in S2 cells were performed as described previously (41). In dsRNA-induced RNAi reporter assays with individual proteins, S2 cells in 96-well plates were transfected with 12.5 ng of pMT-FLuc, 3 ng of pMT-RLuc and 50 ng of an expression plasmid for one of the viral proteins using Effectene Transfection Reagent (QIAGEN). Two days after transfection, 1.4 ng/ μ l of dsRNA was added to the culture supernatant. Expression of the luciferase reporters was induced the same day with 0.5 mM of CuSO₄. Luciferase activities were measured the following day with the Dual-Luciferase Reporter Assay System (Promega). The siRNA-induced RNAi reporter assays with individual proteins were performed as two variants. One of these variants was identical to the dsRNA-induced RNAi reporter assay, except that dsRNA feeding was omitted and siRNAs (2 pmol) were co-transfected with the plasmids. In the other variant, S2 cells in 24-well plates were transfected with 100 ng of pCoBlast (Life Technologies) and 300 ng of an expression plasmid for one of the viral proteins. Two days after transfection, the cells were transferred to 96-well plates and the culture medium was supplemented with 25 μ g/ml of blasticidin S (Life Technologies) to select for cells that express the viral proteins. The cells were transfected the following day with 12.5 ng of pMT-FLuc, 3 ng of pMT-RLuc, 2 pmol of siRNAs and 50 ng of a carrier plasmid. The reporters were induced the next day and luciferase activities were measured one day after induction. In RNAi reporter assays with infected cells, mock- and CYV-infected S2 cells in 96-well plates were transfected 3 days post-infection with 12.5 ng of pMT-FLuc, 3 ng of pMT-RLuc and either 10 ng of dsRNA or 2 pmol of siRNAs. Expression of the luciferase reporters was induced the same day and luciferase activities were measured 4 days post-infection. RNAi reporter assays with DXV-infected S2 cells were performed in a similar fashion, except that transfection and induction were performed at 6 h and 1 day post-infection, respectively. Luciferase activities were measured 2 days post-infection.

For RNAi reporter assays in CT cells, mock- and CYV-infected CT cells in 24-well plates were transfected 2 days post-infection with 250 ng of pAc-FLuc, 250 ng of pAc-RLuc and 10 ng of dsRNA using X-tremeGENE HP DNA Transfection Reagent (Roche). Luciferase activities were measured 2 days post-infection.

FHV RNA1 replicon assay

S2 cells in a 24-well plate were transfected with 100 ng of the wild-type or Δ B2 FHV RNA1 replicons and 300 ng of an expression plasmid for one of the viral proteins using Effectene Transfection Reagent. Transcription of the FHV RNA1 replicons was induced two days after transfection by the addition of 0.5 mM of CuSO₄ to the culture supernatant. The next day, RNA was isolated from the cells using Isol-RNA Lysis Reagent. The RNA was treated with DNase I (Life Technologies) and converted to cDNA using TaqMan Reverse Transcription Reagents (Life Technologies) and either FHV RNA1-specific primer T7-FHV-RNA1-R1 or RpL32-specific primer RpL32-R1 (Supplementary Table S1). The cDNA samples were then used in quantitative PCRs (qPCRs) on a LightCycler 480 (Roche) using GoTaq qPCR Master Mix (Promega) and either primers T7-F1 and FHV-RNA1-F3 (FHV RNA1 qPCR) or primers RpL32-R1 and RpL32-F1 (RpL32 qPCR) (Supplementary Table S1). The FHV RNA1 data were normalized to RpL32.

Dicer assays, Slicer assays and electrophoretic mobility shift assays (EMSAs)

Dicer assays, Slicer assays and EMSAs with purified recombinant proteins and radioactively-labeled probes were done essentially as described previously (2,23,42). Dicer assays were performed in 12- μ l reactions with recombinant proteins, 4 μ l of cell extract and 5 ng of radioactively-labeled 126-nt dsRNA. For Dicer assays in mock- and CYV-infected cell extracts, recombinant proteins were omitted from the reaction. Dicer assays in S2 cell extracts were incubated for 3 h at 25°C and those in U4.4, CT and Hsu cell extracts at 28°C. The reactions were treated with proteinase K (Life Technologies), extracted with phenol/chloroform, precipitated and analyzed on 12% denaturing polyacrylamide gels.

Slicer assays were done in 11- μ l reactions that contained 5 μ l of *D. melanogaster* embryo lysate and 50 nM of siRNAs. The siRNA duplexes were first incubated in the embryo lysates for 30 min at 25°C to allow assembly of mature RISC. Recombinant proteins were then added and the incubation was continued for another 30 min before the reactions were supplemented with the radioactive 5' cap-labeled 492-bp target RNA. The reactions were incubated for an additional 2 h at 25°C before they were treated with proteinase K, extracted with phenol/chloroform, precipitated and analyzed on an 8% denaturing polyacrylamide gel.

EMSAs were performed in 16- μ l reactions with recombinant proteins and either 5 ng of radioactively-labeled 126-nt dsRNA or 1 nM of radioactively-labeled 21-nt siRNA, 21-nt dsRNA, 19-nt dsRNA, 23-nt microRNA (miRNA) or 21-nt dsDNA duplexes. The reactions were incubated for 1 h at room temperature and analyzed on 6% (126-nt dsRNA) and 8% (small RNA and DNA duplexes) native polyacrylamide gels.

Dicer assays, Slicer assays and EMSAs were visualized by autoradiography using KODAK BioMax XAR films. To quantify the fraction bound probe in the EMSAs, the radioactive signals were captured with a Molecular Imager

FX (Bio-Rad) and quantified with ImageJ (version 1.47k) (43).

Statistics

IBM SPSS Statistics (version 20) was used to statistically analyze the data. Statistical significance was addressed by applying an unpaired *t*-test or, in the case of multiple comparisons, a one-way ANOVA followed by a Dunnett's *post hoc* test.

RESULTS

CYV is a target of the *Culex* RNAi machinery

The identification of vsiRNAs in infections with DXV, *Drosophila* birnavirus and Mosquito X virus as well as the enhanced sensitivity of *R2D2* and *AGO2* mutant flies to DXV infection indicates that entomobirnaviruses are a target of the antiviral RNAi machinery in insects (14,29,44,45). To investigate whether the *Culex* RNAi machinery targets CYV, we first analyzed whether CYV efficiently replicates in *C. quinquefasciatus* Hsu and *C. tarsalis* CT cells. Since Hsu cells were resistant to CYV (data not shown), we performed massive parallel sequencing of the small RNAs in CYV-infected CT cells. The small RNAs were mapped to the viral genome allowing one mismatch during alignment to account for genome variants that result from the relatively high error rates generally observed for viral RNA-dependent RNA polymerases. We detected 10 260 120 small RNAs that mapped to the viral genome. These viral small RNAs were almost exclusively 21 nt in length (Figure 1A), a hallmark of siRNAs that are generated by Dcr-2. The majority of the 21-nt vsiRNAs (9 001 430 in total; 6 997 378 and 2 004 052 for segments A and B, respectively) mapped across the entire length of the viral genome (Figure 1B). In addition, we noted a clear vsiRNA hotspot on the 3' end of the (–) strand of both genome segments (Figure 1B). Overall, however, the vsiRNAs did not display a clear strand bias, as they mapped in similar numbers to the sense strand (46% for segment A and 47% for segment B) and antisense strand (54% for segment A and 53% for segment B) (Figure 1B). These results indicate that CYV is exposed to an RNAi response in *Culex* cells and they suggest that the CYV dsRNA genome is the major Dcr-2 substrate for vsiRNA production. Similar results were obtained when restricting the analyses to the 9 875 389 small RNAs that mapped to the viral genome without mismatches (data not shown).

The CYV VP3 protein suppresses RNAi

Since CYV is a target of the antiviral RNAi machinery in *Culex*, we deemed it likely that the virus would encode a VSR. We therefore used well-established reporter assays to determine whether CYV counteracts RNAi (41). In these assays, the effect of virus infection or expression of individual viral proteins on RNAi-mediated silencing of a firefly luciferase (FLuc) reporter is monitored. We first determined whether RNAi is suppressed in cells that are infected with CYV. To this end, we measured luciferase activities in mock- and CYV-infected cells that were co-transfected with

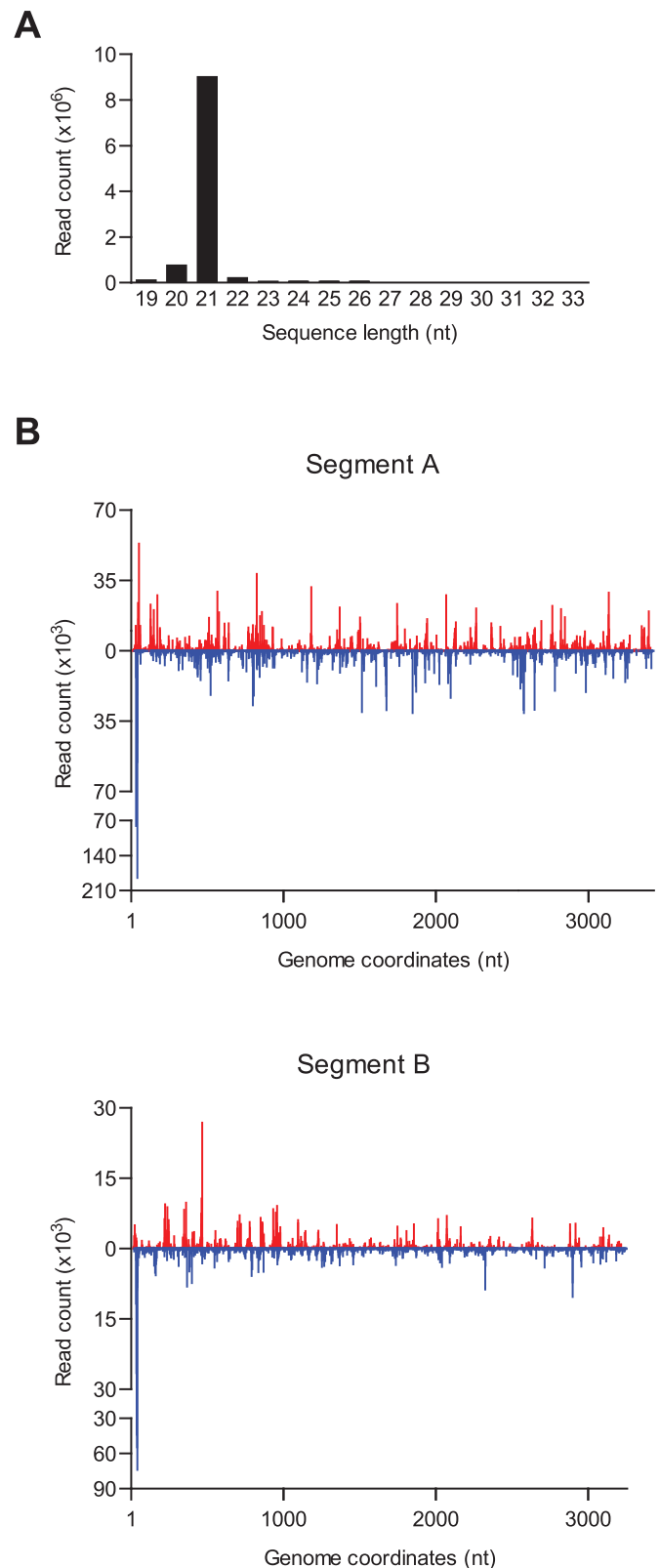


Figure 1. CYV is targeted by the *Culex* RNAi machinery. (A) Size profile of viral small RNAs in CYV-infected CT cells. The small RNAs were mapped to the CYV genome allowing one mismatch. (B) Distribution of the vsiRNAs over the CYV genome. The 21-nt vsiRNAs in CYV-infected CT cells were aligned to CYV genome segments A (upper panel) and B (lower panel). Small RNAs that map to the (+) strand of the viral genome are shown in red and those that map to the (–) strand in blue.

the FLuc reporter plasmid and 113-nt *in vitro* transcribed FLuc dsRNA. A *Renilla* luciferase (RLuc) reporter plasmid was included as a normalization control. As expected, in mock-infected *Drosophila* S2 cells, the FLuc reporter was efficiently silenced (~600-fold) by dsRNA treatment (Figure 2A, left panel). However, dsRNA-mediated silencing of the FLuc reporter was strongly suppressed (to ~6-fold; $P = 0.002$) in CYV-infected S2 cells (Figure 2A, left panel). A comparable reduction of FLuc silencing (from ~300-fold to ~20-fold; $P < 0.001$) was observed in CYV-infected *Culex* CT cells (Figure 2A, right panel). CYV infection also suppressed silencing of the FLuc reporter (from ~15-fold to ~3-fold; $P = 0.025$) when we induced RNAi with 21-nt synthetic siRNA duplexes (Figure 2B). These data show that CYV infection inhibits RNAi induced by dsRNA as well as siRNAs.

To identify the viral proteins responsible for CYV-mediated RNAi suppression, we generated expression constructs for the five proteins (VP1 to VP5) that are predicted to be encoded by the CYV genome (Figure 3A). Expression of all five proteins in transfected cells was confirmed by western blot analysis (Figure 3B). We then tested the individual viral proteins for VSR activity in our RNAi reporter assays. Cells were co-transfected with the FLuc and RLuc reporter plasmids and an expression plasmid for one of the viral proteins. The FLuc reporter was silenced by dsRNA feeding two days after transfection to allow expression of the viral proteins before the induction of RNAi. Of the five viral proteins, only VP3 suppressed silencing of the FLuc reporter (from ~15-fold to background levels; $P < 0.001$) to a similar extent as the positive control CrPV 1A (22) (Figure 3C). However, VP3 did not inhibit silencing of the FLuc reporter when RNAi was induced by co-transfection of siRNAs along with the luciferase and VP3 expression plasmids (Figure 3D). This is in contrast to the AGO2 antagonists Nora virus VP1 ($P = 0.002$) and CrPV 1A that effectively suppress siRNA-induced RNAi in reporter assays (Figure 3D and (22,23)). The inability of VP3 to suppress siRNA-induced RNAi under these conditions seems at odds with the reduced efficiency of siRNA-induced RNAi in CYV-infected cells (Figure 2B). However, in Figure 2B, the cells were infected three days prior to transfection of the siRNAs and reporter plasmids, whereas in Figure 3D, the siRNAs were co-transfected along with the luciferase and VP3 expression plasmids. Most likely, the siRNAs are incorporated into RISC before VP3 is expressed at sufficiently high levels in the latter case. Indeed, VP3 was able to suppress silencing of the FLuc reporter (from ~27-fold to ~13-fold; $P < 0.001$) when the VP3 expression plasmid was transfected three days before transfection of the siRNAs and reporter plasmids (Figure 3E). These data suggest that VP3 suppresses the RNAi pathway at a step that precedes target cleavage by AGO2.

The RNAi pathway shares basic features with the miRNA pathway. Both pathways depend on Dicer proteins for the generation of small RNAs that guide the recognition and silencing of complementary RNAs by Argonaute proteins. The Dicer and Argonaute proteins in the RNAi and miRNA pathways are, however, different. The RNAi pathway depends on Dcr-2 and AGO2 for small RNA biogenesis and function, whereas the miRNA pathway predominantly

depends on Dcr-1 and AGO1. We observed that CYV VP3 did not interfere with miRNA biogenesis and function (see Supplementary Data), indicating that VP3 specifically inhibits the RNAi pathway.

The VSR activity of VP3 is conserved in DXV

Having identified CYV VP3 as a suppressor of RNAi, we analyzed whether the VSR activity of this protein is conserved in DXV, an entomobirnavirus that infects *Drosophila*. To this end, we first studied RNAi suppression in DXV-infected cells. As observed for CYV, dsRNA-mediated silencing of the FLuc reporter was strongly suppressed (from ~1300-fold to ~150-fold; $P = 0.005$) in S2 cells infected with DXV (Figure 4A). We then tested the DXV VP3 protein for VSR activity. DXV VP3 suppressed silencing of the FLuc reporter (from ~15-fold to background levels; $P < 0.001$) when RNAi was induced by dsRNA feeding two days after transfection of the luciferase and VP3 expression plasmids (Figure 4B). In addition, DXV VP3 suppressed silencing of the FLuc reporter (from ~23-fold to ~9-fold; $P < 0.001$) when we induced RNAi by co-transfection of siRNAs along with the luciferase and VP3 expression plasmids (Figure 4C), and (from ~19-fold to ~3-fold; $P < 0.001$) when the siRNAs and reporter plasmids were transfected three days after transfection of the VP3 expression plasmid (Figure 4D). These results indicate that the VSR activity of VP3 is conserved during entomobirnavirus evolution.

CYV and DXV VP3 can functionally replace FHV B2

Our data indicate that the CYV and DXV VP3 proteins are functional RNAi suppressors. Reverse genetics systems to engineer entomobirnaviruses are not yet available, precluding us to study the importance of VP3's VSR activity in an authentic infection. As an alternative, we tested whether the entomobirnavirus VP3 proteins can functionally replace B2, the well-established VSR of FHV (5,20,21,46). The bisegmented FHV genome consists of genomic RNA1 and RNA2, which encode the RNA-dependent RNA polymerase (protein A) and capsid proteins, respectively. In addition to encoding the RNA-dependent RNA polymerase, RNA1 gives rise to subgenomic RNA3, which encodes the RNAi suppressor protein B2. FHV RNA1 can replicate autonomously, but its replication in RNAi competent insect cells is severely restricted in the absence of B2 (4,46). The replication defect of B2-deficient FHV RNA1 is attributed to its inability to suppress the antiviral RNAi response, since its replication is restored by suppression of the RNAi pathway (4,46).

We used an FHV RNA1 Δ B2 replicon to determine whether the CYV and DXV VP3 proteins can rescue its replication. This FHV RNA1 Δ B2 replicon contains two point mutations in the B2 coding region (Figure 5A). These point mutations disrupt B2, but they do not affect the amino acid sequence of the RNA-dependent RNA polymerase (47). We co-transfected cells with the FHV RNA1 Δ B2 replicon and one of the VP3 expression plasmids and monitored RNA1 accumulation. As predicted, FHV RNA1 Δ B2 was severely impaired when compared to wild-type FHV

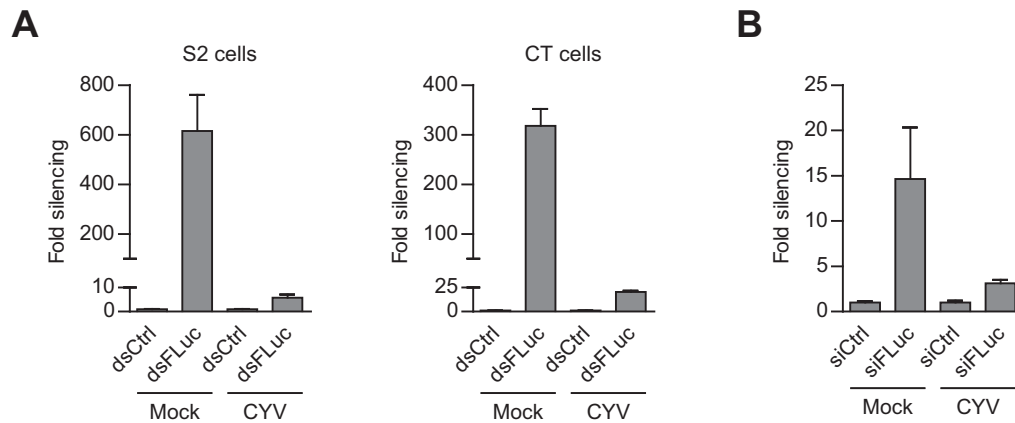


Figure 2. RNAi is suppressed during CYV infection. (A) dsRNA-induced RNAi reporter assays in infected *Drosophila* S2 (left panel) and *Culex* CT (right panel) cells. Firefly (FLuc) and *Renilla* (RLuc) luciferase expression plasmids were transfected together with non-specific control (dsCtrl) or FLuc (dsFLuc) dsRNA into mock- and CYV-infected cells. Luciferase activities were measured and FLuc counts were normalized to RLuc counts. The data are presented as fold silencing relative to dsCtrl. (B) siRNA-induced RNAi reporter assay in infected S2 cells. The experiment was performed as in (A), except that RNAi was induced by co-transfection of non-specific control (siCtrl) or FLuc (siFLuc) siRNAs along with the luciferase expression plasmids. The data are presented as fold silencing relative to siCtrl. Bars and error bars in all panels represent the mean and standard deviation of three independent samples.

RNA1. The RNA1 levels of the B2-deficient replicon only reached 0.15% of those of the wild-type replicon, a difference of ~700-fold. However, replication of the B2-deficient replicon was enhanced in the presence of our positive control Nora virus VP1 (23) (~100-fold; to 15% of the wild-type replicon; $P = 0.041$), and in the presence of either CYV or DXV VP3 (~200-fold; to 34% of the wild-type replicon; $P < 0.001$ for both) (Figure 5B). These results show that entomobirnavirus VP3 proteins can functionally replace the VSR of FHV.

CYV and DXV VP3 inhibit dicing of dsRNA

VSRs of different viruses may target different aspects of the RNAi machinery, such as Dcr-2-mediated cleavage of dsRNA and slicing of target RNAs by AGO2. To characterize the VSR activity of CYV and DXV VP3 in more detail, we performed a series of biochemical assays using maltose-binding protein (MBP)-tagged recombinant proteins purified from *Escherichia coli*. We first tested whether the recombinant VP3 proteins interfere with dicing of dsRNA, the initiation phase of the RNAi pathway. We incubated radioactively-labeled 126-nt dsRNA in *D. melanogaster* S2, *A. albopictus* U4.4, *C. quinquefasciatus* Hsu and *C. tarsalis* CT cell extracts and monitored its processing into 21-nt siRNAs on denaturing polyacrylamide gels. The dsRNA was efficiently processed into siRNAs in extracts from all cell types (Figure 6A, lanes 10, 15, 20 and 25). Processing of the dsRNA was, however, inhibited in a dose-dependent manner by the VP3 proteins of both CYV (Figure 6A, lanes 6–8, 11–13, 16–18 and 21–23) and DXV (Figure 6A, lanes 3–5), and in the presence of DCV 1A (Figure 6A, lane 1), a VSR that is known to interact with dsRNA (2). As expected, MBP alone did not inhibit dsRNA processing (Figure 6A, lanes 9, 14, 19 and 24). These data indicate that the entomobirnavirus VP3 proteins interfere with siRNA production by Dcr-2. Importantly, inhibition of dsRNA cleavage into siRNAs was also observed in extracts from *Drosophila* S2 and *Culex* CT cells infected with CYV. The dsRNA was

processed in extracts from mock-infected cells (Figure 6B, lanes 5 and 10), but no dsRNA processing was observed in extracts from CYV-infected cells (Figure 6B, lanes 1 and 6). Titration of CYV-infected cell extracts into mock-infected cell extracts abolished dsRNA processing (Figure 6B, lanes 2–4 and 7–9), which confirms the presence of a Dcr-2 inhibitor in CYV-infected cells.

We next tested whether the recombinant VP3 proteins are capable of interfering with slicing of target RNAs, the effector phase of the RNAi pathway. For this purpose, a radioactive 5' cap-labeled target RNA, containing 492 nt of the FLuc coding sequence, was incubated in *D. melanogaster* embryo extracts in the presence of a FLuc-specific siRNA that triggers its cleavage. Cleavage of the target RNA results in the production of a 164-nt 5' cleavage product that can be visualized on a denaturing polyacrylamide gel. As expected, cleavage of the target RNA was induced by the FLuc-specific siRNA (Figure 6C, lane 2), but not by a non-specific control siRNA (Figure 6C, lane 1). Neither MBP alone (Figure 6C, lanes 3, 4 and 12), nor the VP3 proteins of CYV (Figure 6C, lanes 5–7) or DXV (Figure 6C, lanes 8–10), inhibited target RNA cleavage. Complete inhibition of target RNA cleavage was, however, seen in the presence of the positive control Nora virus VP1 (Figure 6C, lane 11), an established VSR that interferes with the Slicer activity of AGO2 (23). These results demonstrate that the entomobirnavirus VP3 proteins do not interfere with target RNA cleavage by AGO2.

CYV and DXV VP3 possess dsRNA- and siRNA-binding activity

Many VSRs employ dsRNA binding as a mechanism to suppress RNAi (8,9). The ability of the entomobirnavirus VP3 proteins to inhibit Dcr-2-mediated cleavage of dsRNA into siRNAs suggests a similar strategy of RNAi suppression. To study whether these proteins indeed possess dsRNA-binding activity, we performed EMSAs using

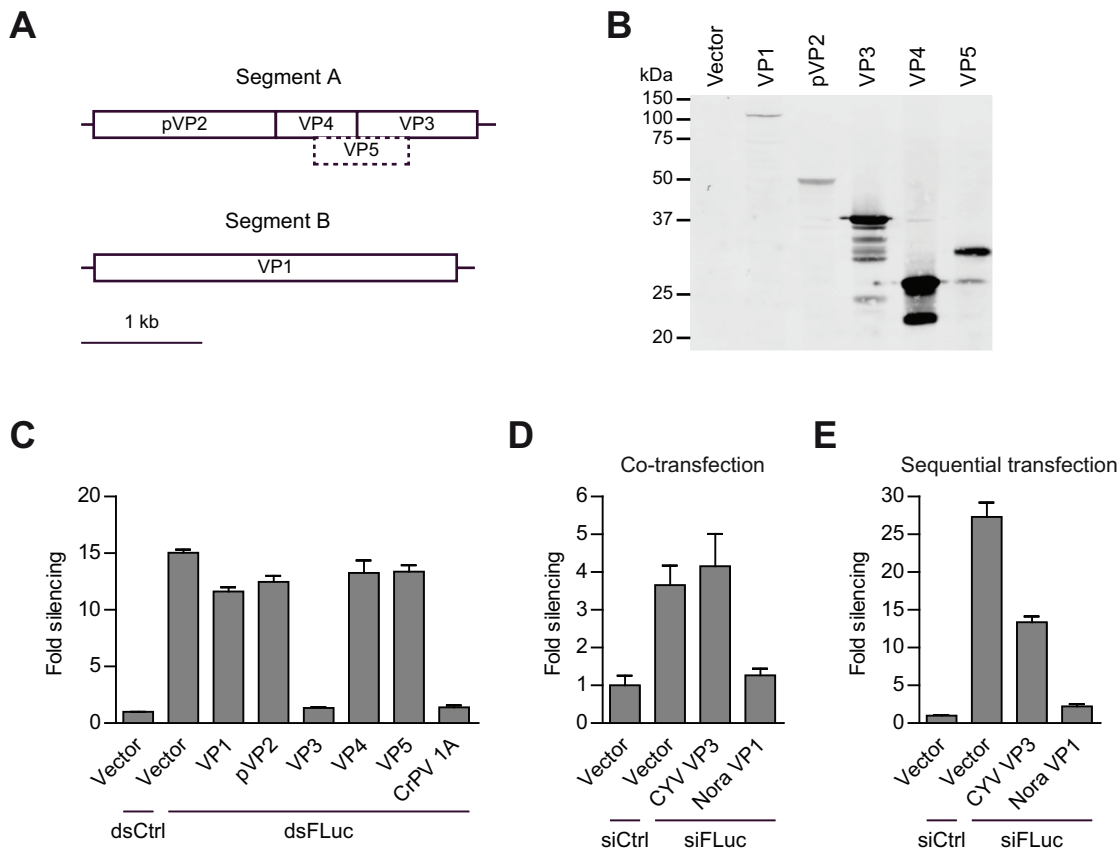


Figure 3. CYV VP3 suppresses RNAi. (A) Schematic representation of the bisegmented dsRNA genome of CYV. Genome segment A encodes a polyprotein precursor of pVP2 (capsid precursor), VP4 (protease) and VP3 (ribonucleoprotein). A VP5 protein, homologous to DXV VP5, might be expressed from the -1 reading frame. Unlike DXV VP5, which initiates from a canonical AUG codon, expression of CYV VP5 would require initiation from a non-AUG codon. To ensure efficient expression, we introduced an AUG start codon in the CYV VP5 expression plasmid. Genome segment B encodes the RNA-dependent RNA polymerase VP1. (B) Western blot analysis of CYV protein expression. S2 cells were transfected with a plasmid encoding one of the CYV proteins (VP1 to VP5) fused to the V5-epitope tag and protein expression was analyzed by western blot using anti-V5 antibodies. (C) dsRNA-induced RNAi reporter assay in S2 cells. Firefly (FLuc) and *Renilla* (RLuc) luciferase expression plasmids were transfected into the cells together with an empty vector control (Vector) or a plasmid encoding one of the CYV proteins (VP1 to VP5). An expression plasmid for CrPV 1A was used as positive control. Two days after transfection, the cells were soaked in medium containing non-specific control (dsCtrl) or FLuc (dsFLuc) dsRNA. Luciferase activities were measured and FLuc counts were normalized to RLuc counts. The data are presented as fold silencing relative to dsCtrl. (D) and (E) siRNA-induced RNAi reporter assays in S2 cells. The experiments were done as in (C), except that RNAi was induced with non-specific control (siCtrl) or FLuc (siFLuc) siRNAs. In (D), the siRNAs were co-transfected along with the expression plasmids for the luciferases and the viral proteins, whereas in (E), the siRNAs and luciferase expression plasmids were co-transfected three days after transfection of the plasmids that encode the viral proteins. An expression plasmid for Nora virus VP1 (Nora VP1) was used as positive control. The data are presented as fold silencing relative to siCtrl. Bars and error bars in (C) to (E) represent the mean and standard deviation of three independent samples.

the recombinant VP3 proteins and different radioactively-labeled probes.

First, we incubated 126-nt blunt dsRNA with serial dilutions of the recombinant VP3 proteins and resolved dsRNA-protein complexes on native polyacrylamide gels. As expected, incubation of dsRNA with MBP alone (Figure 7A, lane 15) did not alter its mobility when compared to the control reaction without recombinant protein (Figure 7A, lane 16). However, the mobility of the dsRNA was inhibited in a dose-dependent manner by the VP3 proteins of both CYV (Figure 7A, lanes 8–14) and DXV (Figure 7A, lanes 1–7). CYV and DXV VP3 displayed similar affinities for dsRNA, with dissociation constants of 115.6 ± 24.5 and 166.1 ± 33.2 nM, respectively (Figure 7A).

The dsRNA-binding activity of the entomobirnavirus VP3 proteins most likely suppresses RNAi by inhibiting

dsRNA processing by Dcr-2. However, inhibition of siRNA production cannot fully explain the RNAi-suppressive activity of the VP3 proteins, since they suppressed siRNA-induced RNAi in our reporter assays (Figures 3E and 4D). This observation indicates that these proteins target additional steps of the RNAi pathway, such as loading of siRNAs into RISC or slicing of target RNAs by AGO2. Since our biochemical assays indicate that the VP3 proteins do not interfere with the AGO2 Slicer activity (Figure 6C), we tested whether these proteins have the potential to scavenge siRNAs to prevent their incorporation into RISC. To this end, we tested serial dilutions of the recombinant VP3 proteins in EMSAs with 21-nt siRNA duplexes containing 2-nt 3' overhangs. When compared to the control reaction without recombinant protein (Figure 7B, lane 16), the mobility of the siRNAs was inhibited in a dose-dependent manner

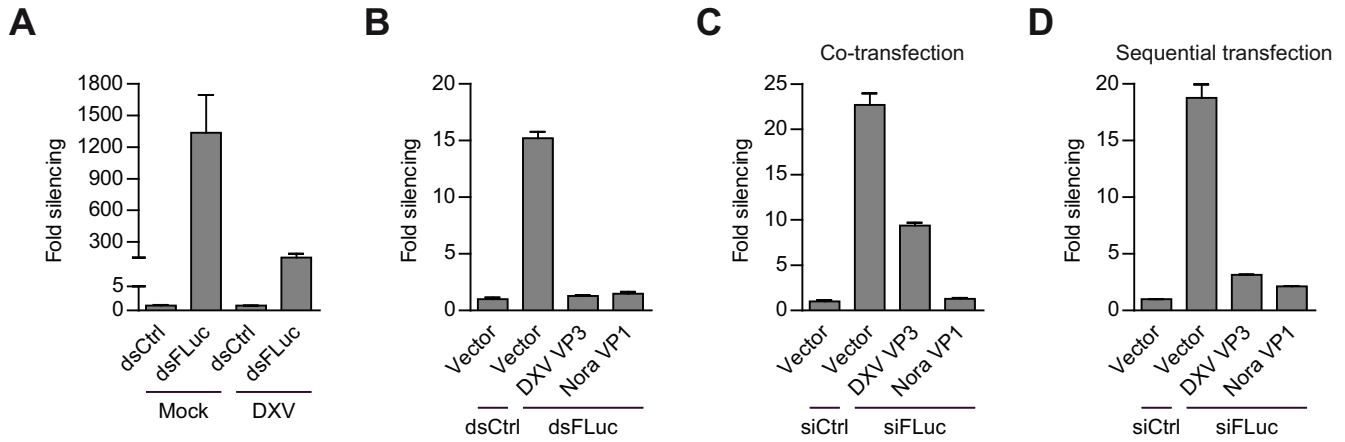


Figure 4. DXV VP3 suppresses RNAi. (A) dsRNA-induced RNAi reporter assay in infected S2 cells. The assay was performed with DXV as described for CYV in the legend to Figure 2A. (B) dsRNA-induced and (C) and (D) siRNA-induced RNAi reporter assays in S2 cells. The experiments were done as described in the legends to Figure 3C, D and E, respectively, but with a plasmid encoding DXV VP3. An expression plasmid for Nora virus VP1 (Nora VP1) was used as positive control. Bars and error bars in all panels represent the mean and standard deviation of three independent samples.

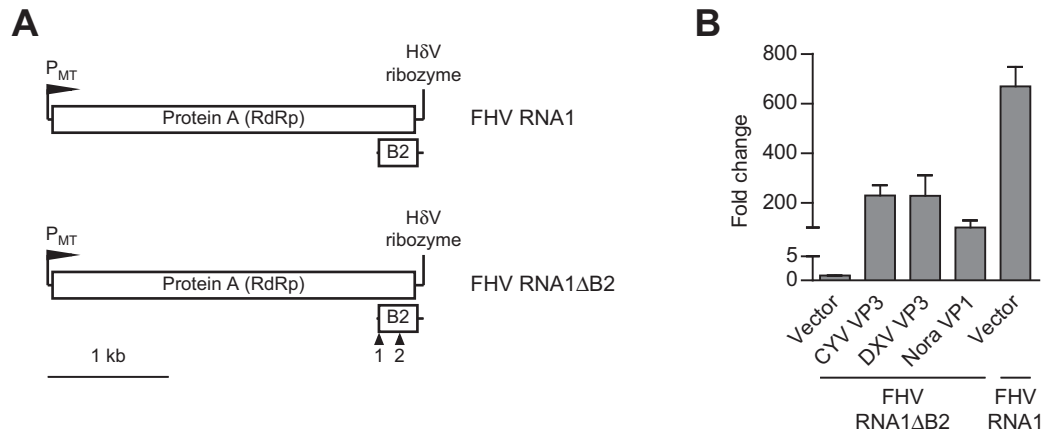


Figure 5. CYV and DXV VP3 rescue replication of a B2-deficient FHV RNA1 replicon. (A) Schematic representations of FHV RNA1 and FHV RNA1 Δ B2. The replicons are launched from a copper-inducible metallothionein promoter (P_{MT}). Their 3' end is defined by a Hepatitis delta virus (H δ V) ribozyme. Mutations in the B2 coding sequence are indicated by arrow heads. Mutation 1 (T2739C; with respect to the FHV RNA1 sequence; GenBank accession number: X77156.1) disrupts the AUG start codon and mutation 2 (C2910A) introduces a premature UAA stop codon. RdRp, RNA-dependent RNA polymerase (B) FHV RNA1 replicon assay in S2 cells. The FHV RNA1 Δ B2 replicon was transfected into the cells together with an empty vector control (Vector) or a plasmid encoding either CYV or DXV VP3. An expression plasmid for Nora virus VP1 (Nora VP1) was used as positive control. The wild-type FHV RNA1 replicon was transfected together with the empty vector control to indicate wild-type replication levels. FHV RNA1 replication levels were quantified by qPCR and normalized to RpL32. The data are presented as fold change relative to FHV RNA1 Δ B2 co-transfected with the empty vector control. Bars and error bars in (B) represent the mean and standard deviation of three independent samples.

after incubation with the VP3 proteins of both CYV (Figure 7B, lanes 8–14) and DXV (Figure 7B, lanes 1–7), but not after incubation with MBP alone (Figure 7B, lane 15). As for long dsRNA, CYV and DXV VP3 showed similar affinities for siRNAs, with dissociation constants of 2.6 ± 1.4 and 5.9 ± 1.6 μ M, respectively (Figure 7B). Interestingly, both proteins also bound 21- and 19-nt blunt dsRNA, but only showed weak binding to a 23-nt miRNA duplex (Figure 7C), consistent with the observation that VP3 does not inhibit the miRNA pathway (Supplementary Figure S1B). Binding was RNA-specific, as neither VP3 protein was able to interact with 21-nt blunt dsDNA (Figure 7C). Taken together, our data indicate that the entomobirnavirus VP3 proteins are RNAi suppressors that bind both long dsRNA as well as siRNAs. The dsRNA-binding activity of the VP3

proteins inhibits dsRNA processing into siRNAs and, presumably, loading of siRNAs into RISC.

DISCUSSION

Viruses employ many different strategies to suppress or evade the innate and adaptive immune responses of their hosts. In arthropods, RNAi has antiviral activity against all major classes of insect viruses, including (+) and (–) strand RNA, dsRNA and DNA viruses (2–4,14–19,30–32). Nevertheless, RNAi suppression has thus far not been detected in infections with dsRNA viruses. How widespread viral RNAi antagonism is among different classes of viruses remains unclear. Here, we show that the antiviral RNAi pathway is inhibited during infections with mosquito

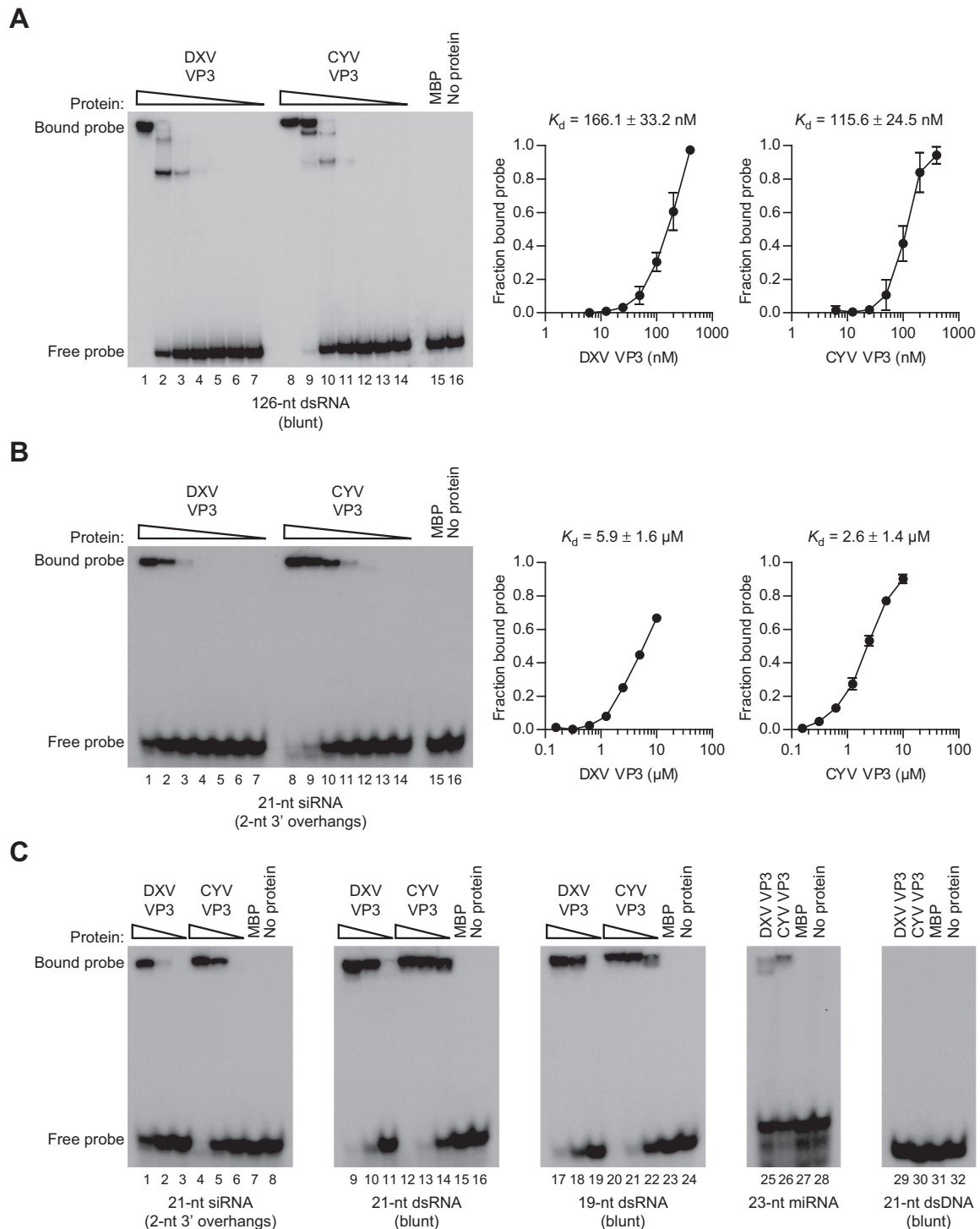


Figure 7. CYV and DXV VP3 bind dsRNA independent of length. (A) EMSA with 126-nt dsRNA. Radioactively-labeled dsRNA was incubated with MBP-tagged CYV or DXV VP3. MBP alone served as negative control. The reactions were separated on a native polyacrylamide gel and visualized by autoradiography (left panel). The EMSA is representative for three independent experiments. The fraction bound probe was quantified for each protein concentration and used to calculate the K_d (right panels). Data points and error bars represent the mean and standard deviation of samples from the three independent experiments. Protein concentrations were as follows: 2-fold dilutions starting at 400 nM for CYV VP3 (lanes 8–14) and DXV VP3 (lanes 1–7); 400 nM for MBP (lane 15). A reaction with buffer instead of recombinant protein (No protein; lane 16) was used to mark the position of the free probe. (B) EMSA with 21-nt siRNAs. The assay was performed as in (A), but protein concentrations were as follows: 2-fold dilutions starting at 10 μ M for CYV VP3 (lanes 8–14) and DXV VP3 (lanes 1–7); 10 μ M for MBP (lane 15). (C) EMSAs with different RNA and DNA probes. In the 21-nt siRNA (first panel), 21-nt dsRNA (second panel) and 19-nt dsRNA (third panel) EMSAs, 4-fold dilutions starting at 10 μ M of CYV VP3 (lanes 4–6, 12–14 and 20–22) and DXV VP3 (lanes 1–3, 9–11 and 17–19) were tested. In the 23-nt miRNA (fourth panel) and 21-nt dsDNA (fifth panel) EMSAs, CYV VP3 (lanes 26 and 30) and DXV VP3 (lanes 25 and 29) were analyzed at a concentration of 10 μ M. The concentration of MBP (lanes 7, 15, 23, 27 and 31) was 10 μ M in all EMSAs.

the other *Birnaviridae* genera, nor could we identify known nucleic acid-binding motifs using online domain prediction programs. Whether entomobirnavirus VP3 has structural similarity to other dsRNA-binding proteins or whether it uses a novel protein fold for dsRNA binding is an open question for future investigation.

In principle, any dsRNA-binding protein has the potential to inhibit RNAi when overexpressed. Even a dsRNA-binding protein from *E. coli*, a species that is not targeted by an RNAi response, is able to suppress RNAi under overexpression conditions (53). It has been shown previously that the IBDV, IPNV and DXV VP3 proteins have the capacity to suppress RNAi (54). However, these studies were done in a heterologous system and the *in vivo* relevance in a relevant host remained unclear. Our study now provides evidence that both CYV and DXV infections suppress the RNAi response in insect cells and that their VP3 proteins are *bona fide* RNAi suppressors that rescue replication of a VSR-defective FHV RNA1 replicon.

dsRNA is an important activator of innate immune pathways, such as the interferon response in vertebrates and antiviral RNAi in invertebrates. To avoid recognition by the host's immune system, viruses have evolved different mechanisms to shield their dsRNA. The genomes of most dsRNA viruses, for example, are replicated in specialized viral cores that encapsulate the dsRNA genome throughout the viral replication cycle (55). These viral cores are common among dsRNA viruses, but they are absent from birnaviruses. Instead, studies with IBDV and IPNV have shown that birnaviruses form ribonucleoprotein (RNP) complexes consisting of the dsRNA genome and the VP1 and VP3 proteins (56,57). Since VP3 binds homogeneously along the dsRNA genome, the RNP complexes are thought to prevent the activation of cellular immune pathways. Our observation that the VP3 proteins of CYV and DXV inhibit RNAi by dsRNA binding supports this hypothesis. Entomobirnaviruses most likely form similar RNP complexes that shield the viral genome from the antiviral activity of the RNAi pathway. Nevertheless, we found that vsRNAs, derived from the viral genome, are produced in CYV-infected cells. Moreover, vsRNAs were previously detected in cells infected with DXV, *Drosophila* birnavirus and Mosquito X virus (29,44,45). These data imply that some of the entomobirnaviral dsRNA is accessible for Dcr-2. The observation that dsRNA viruses from the *Totiviridae* and *Reoviridae* families are also prone to an RNAi response shows that the protection of dsRNA by other dsRNA viruses is incomplete as well (44,58,59). By RNP complex formation, VP3 probably limits the accessibility of the viral genome for Dcr-2, but it cannot prevent that some viral dsRNA feeds into the RNAi pathway and is processed into siRNAs. These siRNAs may be loaded into RISC, where they guide cleavage of single-stranded viral transcripts, thereby adding another level of antiviral activity. However, we observed that the CYV and DXV VP3 proteins do not only bind long dsRNA, but also siRNA duplexes. These data suggest that VP3 does not merely protect the viral genome against Dcr-2, but that it also scavenges siRNAs to prevent their incorporation into RISC. Thus, entomobirnavirus VP3 proteins counteract multiple aspects of the antiviral RNAi machinery.

Complex interactions may be occurring between mosquito-specific viruses, pathogenic arboviruses and their mosquito hosts. For example, induction and suppression of antiviral pathways by mosquito-specific viruses may affect the transmission efficiency of co-infecting arboviruses. The characterization of RNAi antagonists in mosquito-specific viruses will thus contribute to our understanding of the factors that influence arbovirus transmission.

SUPPLEMENTARY DATA

Supplementary Data are available at NAR Online.

ACKNOWLEDGMENTS

We thank members of the R.P.v.R. laboratory for fruitful discussions, Robert Tesh for Hsu cells, Aaron Brault for CT cells, Jean-Luc Imler for DXV and the FHV UAS-RNA1 and UAS-RNA1 Δ B2 plasmids, Esther Schnettler for miRNA sensor plasmids and Carla Saleh for reporter plasmids pAc-FLuc and pAc-RLuc.

FUNDING

VIDI fellowship [864.08.003 to R.P.v.R.] and the Open Program of the Division for Earth and Life Sciences [821.02.028 to R.P.v.R.] of the Netherlands Organization for Scientific Research; Deutsche Forschungsgemeinschaft [JU 2857/1-1 to S.J., VA 827/1-1 to R.P.v.R.] within the DFG Priority Programme SPP 1596. Funding for open access charge: Netherlands Organization for Scientific Research.

Conflict of interest statement. None declared.

REFERENCES

- Hamilton, A.J. and Baulcombe, D.C. (1999) A species of small antisense RNA in posttranscriptional gene silencing in plants. *Science*, **286**, 950–952.
- van Rij, R.P., Saleh, M.C., Berry, B., Foo, C., Houk, A., Antoniewski, C. and Andino, R. (2006) The RNA silencing endonuclease Argonaute 2 mediates specific antiviral immunity in *Drosophila melanogaster*. *Genes Dev.*, **20**, 2985–2995.
- Wang, X.H., Aliyari, R., Li, W.X., Li, H.W., Kim, K., Carthew, R., Atkinson, P. and Ding, S.W. (2006) RNA interference directs innate immunity against viruses in adult *Drosophila*. *Science*, **312**, 452–454.
- Galiana-Arnoux, D., Dostert, C., Schneemann, A., Hoffmann, J.A. and Imler, J.L. (2006) Essential function in vivo for Dicer-2 in host defense against RNA viruses in *Drosophila*. *Nat. Immunol.*, **7**, 590–597.
- Lu, R., Maduro, M., Li, F., Li, H.W., Broitman-Maduro, G., Li, W.X. and Ding, S.W. (2005) Animal virus replication and RNAi-mediated antiviral silencing in *Caenorhabditis elegans*. *Nature*, **436**, 1040–1043.
- Félix, M.A., Ashe, A., Piffaretti, J., Wu, G., Nuez, I., Bécicard, T., Jiang, Y., Zhao, G., Franz, C.J., Goldstein, L.D. *et al.* (2011) Natural and experimental infection of *Caenorhabditis* nematodes by novel viruses related to nodaviruses. *PLoS Biol.*, **9**, e1000586.
- Segers, G.C., Zhang, X., Deng, F., Sun, Q. and Nuss, D.L. (2007) Evidence that RNA silencing functions as an antiviral defense mechanism in fungi. *Proc. Natl. Acad. Sci. U.S.A.*, **104**, 12902–12906.
- Szittyá, G. and Burgyn, J. (2013) RNA interference-mediated intrinsic antiviral immunity in plants. *Curr. Top. Microbiol. Immunol.*, **371**, 153–181.
- Nayak, A., Tassetto, M., Kunitomi, M. and Andino, R. (2013) RNA interference-mediated intrinsic antiviral immunity in invertebrates. *Curr. Top. Microbiol. Immunol.*, **371**, 183–200.
- Li, Y., Lu, J., Han, Y., Fan, X. and Ding, S.W. (2013) RNA interference functions as an antiviral immunity mechanism in mammals. *Science*, **342**, 231–234.

11. Maillard, P.V., Ciaudo, C., Marchais, A., Li, Y., Jay, F., Ding, S.W. and Voinnet, O. (2013) Antiviral RNA interference in mammalian cells. *Science*, **342**, 235–238.
12. Vijayendran, D., Airs, P.M., Dolezal, K. and Bonning, B.C. (2013) Arthropod viruses and small RNAs. *J. Invertebr. Pathol.*, **114**, 186–195.
13. Bronkhorst, A.W. and van Rij, R.P. (2014) The long and short of antiviral defense: small RNA-based immunity in insects. *Curr. Opin. Virol.*, **7**, 19–28.
14. Zambon, R.A., Vakharia, V.N. and Wu, L.P. (2006) RNAi is an antiviral immune response against a dsRNA virus in *Drosophila melanogaster*. *Cell. Microbiol.*, **8**, 880–889.
15. Mueller, S., Gausson, V., Vodovar, N., Deddouch, S., Troxler, L., Perot, J., Pfeffer, S., Hoffmann, J.A., Saleh, M.C. and Imler, J.L. (2010) RNAi-mediated immunity provides strong protection against the negative-strand RNA vesicular stomatitis virus in *Drosophila*. *Proc. Natl. Acad. Sci. U.S.A.*, **107**, 19390–19395.
16. Han, Y.H., Luo, Y.J., Wu, Q., Jovel, J., Wang, X.H., Aliyari, R., Han, C., Li, W.X. and Ding, S.W. (2011) RNA-based immunity terminates viral infection in adult *Drosophila* in the absence of viral suppression of RNA interference: characterization of viral small interfering RNA populations in wild-type and mutant flies. *J. Virol.*, **85**, 13153–13163.
17. Bronkhorst, A.W., van Cleef, K.W.R., Vodovar, N., Ince, I.A., Blanc, H., Vlak, J.M., Saleh, M.C. and van Rij, R.P. (2012) The DNA virus Invertebrate iridescent virus 6 is a target of the *Drosophila* RNAi machinery. *Proc. Natl. Acad. Sci. U.S.A.*, **109**, E3604–E3613.
18. Kemp, C., Mueller, S., Goto, A., Barbier, V., Paro, S., Bonnay, F., Dostert, C., Troxler, L., Hetru, C., Meignin, C. et al. (2013) Broad RNA interference-mediated antiviral immunity and virus-specific inducible responses in *Drosophila*. *J. Immunol.*, **190**, 650–658.
19. Marques, J.T., Wang, J.P., Wang, X., de Oliveira, K.P.V., Gao, C., Aguiar, E.R.G.R., Jafari, N. and Carthew, R.W. (2013) Functional specialization of the small interfering RNA pathway in response to virus infection. *PLoS Pathog.*, **9**, e1003579.
20. Chao, J.A., Lee, J.H., Chapados, B.R., Debler, E.W., Schneemann, A. and Williamson, J.R. (2005) Dual modes of RNA-silencing suppression by Flock House virus protein B2. *Nat. Struct. Mol. Biol.*, **12**, 952–957.
21. Aliyari, R., Wu, Q., Li, H.W., Wang, X.H., Li, F., Green, L.D., Han, C.S., Li, W.X. and Ding, S.W. (2008) Mechanism of induction and suppression of antiviral immunity directed by virus-derived small RNAs in *Drosophila*. *Cell Host Microbe*, **4**, 387–397.
22. Nayak, A., Berry, B., Tassetto, M., Kunitomi, M., Acevedo, A., Deng, C., Krutchinsky, A., Gross, J., Antoniewski, C. and Andino, R. (2010) Cricket paralysis virus antagonizes Argonaute 2 to modulate antiviral defense in *Drosophila*. *Nat. Struct. Mol. Biol.*, **17**, 547–554.
23. van Mierlo, J.T., Bronkhorst, A.W., Overheul, G.J., Sadanandan, S.A., Ekström, J.O., Heestermans, M., Hultmark, D., Antoniewski, C. and van Rij, R.P. (2012) Convergent evolution of Argonaute-2 slicer antagonism in two distinct insect RNA viruses. *PLoS Pathog.*, **8**, e1002872.
24. Weaver, S.C. and Reisen, W.K. (2010) Present and future arboviral threats. *Antiviral Res.*, **85**, 328–345.
25. Cook, S., Moureau, G., Kitchen, A., Gould, E.A., de Lamballerie, X., Holmes, E.C. and Harbach, R.E. (2012) Molecular evolution of the insect-specific flaviviruses. *J. Gen. Virol.*, **93**, 223–234.
26. Junglen, S. and Drosten, C. (2013) Virus discovery and recent insights into virus diversity in arthropods. *Curr. Opin. Microbiol.*, **16**, 507–513.
27. Marklewitz, M., Gloza-Rausch, F., Kurth, A., Kümmerer, B.M., Drosten, C. and Junglen, S. (2012) First isolation of an Entomobornavirus from free-living insects. *J. Gen. Virol.*, **93**, 2431–2435.
28. Vancini, R., Paredes, A., Ribeiro, M., Blackburn, K., Ferreira, D., Kononchik, J.P. Jr., Hernandez, R. and Brown, D. (2012) Espirito Santo virus: a new birnavirus that replicates in insect cells. *J. Virol.*, **86**, 2390–2399.
29. Huang, Y., Mi, Z., Zhuang, L., Ma, M., An, X., Liu, W., Cao, W. and Tong, Y. (2013) Presence of entomobornaviruses in Chinese mosquitoes in the absence of Dengue virus co-infection. *J. Gen. Virol.*, **94**, 663–667.
30. Keene, K.M., Foy, B.D., Sanchez-Vargas, I., Beaty, B.J., Blair, C.D. and Olson, K.E. (2004) RNA interference acts as a natural antiviral response to O'nyong-nyong virus (Alphavirus; Togaviridae) infection of *Anopheles gambiae*. *Proc. Natl. Acad. Sci. U.S.A.*, **101**, 17240–17245.
31. Campbell, C.L., Keene, K.M., Brackney, D.E., Olson, K.E., Blair, C.D., Wilusz, J. and Foy, B.D. (2008) *Aedes aegypti* uses RNA interference in defense against Sindbis virus infection. *BMC Microbiol.*, **8**, 47.
32. Sánchez-Vargas, I., Scott, J.C., Poole-Smith, B.K., Franz, A.W.E., Barbosa-Solomieu, V., Wilusz, J., Olson, K.E. and Blair, C.D. (2009) Dengue virus type 2 infections of *Aedes aegypti* are modulated by the mosquito's RNA interference pathway. *PLoS Pathog.*, **5**, e1000299.
33. Sullivan, C.S. and Ganem, D. (2005) A virus-encoded inhibitor that blocks RNA interference in mammalian cells. *J. Virol.*, **79**, 7371–7379.
34. Schnettler, E., Sterken, M.G., Leung, J.Y., Metz, S.W., Geertsema, C., Goldbach, R.W., Vlak, J.M., Kohl, A., Khromykh, A.A. and Pijlman, G.P. (2012) Noncoding flavivirus RNA displays RNA interference suppressor activity in insect and mammalian cells. *J. Virol.*, **86**, 13486–13500.
35. Kakumani, P.K., Ponia, S.S., S, R.K., Sood, V., Chinnappan, M., Banerjee, A.C., Medigeshi, G.R., Malhotra, P., Mukherjee, S.K. and Bhatnagar, R.K. (2013) Role of RNA interference (RNAi) in dengue virus replication and identification of NS4B as an RNAi suppressor. *J. Virol.*, **87**, 8870–8883.
36. Scherer, W.F. and Hurlbut, H.S. (1967) Nodamura virus from Japan: a new and unusual arbovirus resistant to diethyl ether and chloroform. *Am. J. Epidemiol.*, **86**, 271–285.
37. Scherer, W.F., Verna, J.E. and Richter, G.W. (1968) Nodamura virus, an ether- and chloroform-resistant arbovirus from Japan: physical and biological properties, with ecologic observations. *Am. J. Trop. Med. Hyg.*, **17**, 120–128.
38. Pijlman, G.P., Funk, A., Kondratieva, N., Leung, J., Torres, S., van der Aa, L., Liu, W.J., Palmenberg, A.C., Shi, P.Y., Hall, R.A. et al. (2008) A highly structured, nuclease-resistant, noncoding RNA produced by flaviviruses is required for pathogenicity. *Cell Host Microbe*, **4**, 579–591.
39. Blankenberg, D., Gordon, A., Von Kuster, G., Coraor, N., Taylor, J., Nekruteno, A. and the Galaxy Team. (2010) Manipulation of FASTQ data with Galaxy. *Bioinformatics*, **26**, 1783–1785.
40. Langmead, B., Trapnell, C., Pop, M. and Salzberg, S.L. (2009) Ultrafast and memory-efficient alignment of short DNA sequences to the human genome. *Genome Biol.*, **10**, R25.
41. van Cleef, K.W.R., van Mierlo, J.T., van den Beek, M. and van Rij, R.P. (2011) Identification of viral suppressors of RNAi by a reporter assay in *Drosophila* S2 cell culture. *Methods Mol. Biol.*, **721**, 201–213.
42. Vodovar, N., Bronkhorst, A.W., van Cleef, K.W.R., Miesen, P., Blanc, H., van Rij, R.P. and Saleh, M.C. (2012) Arbovirus-derived piRNAs exhibit a ping-pong signature in mosquito cells. *PLoS One*, **7**, e30861.
43. Schneider, C.A., Rasband, W.S. and Eliceiri, K.W. (2012) NIH Image to ImageJ: 25 years of image analysis. *Nat. Methods*, **9**, 671–675.
44. Wu, Q., Luo, Y., Lu, R., Lau, N., Lai, E.C., Li, W.X. and Ding, S.W. (2010) Virus discovery by deep sequencing and assembly of virus-derived small silencing RNAs. *Proc. Natl. Acad. Sci. U.S.A.*, **107**, 1606–1611.
45. Vodovar, N., Goic, B., Blanc, H. and Saleh, M.C. (2011) In silico reconstruction of viral genomes from small RNAs improves virus-derived small interfering RNA profiling. *J. Virol.*, **85**, 11016–11021.
46. Li, H., Li, W.X. and Ding, S.W. (2002) Induction and suppression of RNA silencing by an animal virus. *Science*, **296**, 1319–1321.
47. Ball, L.A. (1995) Requirements for the self-directed replication of flock house virus RNA 1. *J. Virol.*, **69**, 720–727.
48. Lombardo, E., Maraver, A., Castón, J.R., Rivera, J., Fernández-Arias, A., Serrano, A., Carrasco, J.L. and Rodríguez, J.F. (1999) VP1, the putative RNA-dependent RNA polymerase of infectious bursal disease virus, forms complexes with the capsid protein VP3, leading to efficient encapsidation into virus-like particles. *J. Virol.*, **73**, 6973–6983.
49. Tacken, M.G.J., Rottier, P.J.M., Gielkens, A.L.J. and Peeters, B.P.H. (2000) Interactions in vivo between the proteins of infectious bursal disease virus: capsid protein VP3 interacts with the RNA-dependent RNA polymerase, VP1. *J. Gen. Virol.*, **81**, 209–218.
50. Tacken, M.G.J., Peeters, B.P.H., Thomas, A.A.M., Rottier, P.J.M. and Boot, H.J. (2002) Infectious bursal disease virus capsid protein VP3 interacts both with VP1, the RNA-dependent RNA polymerase, and with viral double-stranded RNA. *J. Virol.*, **76**, 11301–11311.

51. Oña,A., Luque,D., Abaitua,F., Maraver,A., Castón,J.R. and Rodríguez,J.F. (2004) The C-terminal domain of the pVP2 precursor is essential for the interaction between VP2 and VP3, the capsid polypeptides of infectious bursal disease virus. *Virology*, **322**, 135–142.
52. Pedersen,T., Skjesol,A. and Jørgensen,J.B. (2007) VP3, a structural protein of infectious pancreatic necrosis virus, interacts with RNA-dependent RNA polymerase VP1 and with double-stranded RNA. *J. Virol.*, **81**, 6652–6663.
53. Lichner,Z., Silhavy,D. and Burgyán,J. (2003) Double-stranded RNA-binding proteins could suppress RNA interference-mediated antiviral defences. *J. Gen. Virol.*, **84**, 975–980.
54. Valli,A., Busnadiago,I., Maliogka,V., Ferrero,D., Castón,J.R., Rodríguez,J.F. and García,J.A. (2012) The VP3 factor from viruses of Birnaviridae family suppresses RNA silencing by binding both long and small RNA duplexes. *PLoS One*, **7**, e45957.
55. Ahlquist,P. (2006) Parallels among positive-strand RNA viruses, reverse-transcribing viruses and double-stranded RNA viruses. *Nat. Rev. Microbiol.*, **4**, 371–382.
56. Hjalmarsson,A., Carlemalm,E. and Everitt,E. (1999) Infectious pancreatic necrosis virus: identification of a VP3-containing ribonucleoprotein core structure and evidence for O-linked glycosylation of the capsid protein VP2. *J. Virol.*, **73**, 3484–3490.
57. Luque,D., Saugar,I., Rejas,M.T., Carrascosa,J.L., Rodríguez,J.F. and Castón,J.R. (2009) Infectious bursal disease virus: ribonucleoprotein complexes of a double-stranded RNA virus. *J. Mol. Biol.*, **386**, 891–901.
58. Schnettler,E., Ratinier,M., Watson,M., Shaw,A.E., McFarlane,M., Varela,M., Elliott,R.M., Palmarini,M. and Kohl,A. (2013) RNA interference targets arbovirus replication in *Culicoides* cells. *J. Virol.*, **87**, 2441–2454.
59. Nandety,R.S., Fofanov,V.Y., Koshinsky,H., Stenger,D.C. and Falk,B.W. (2013) Small RNA populations for two unrelated viruses exhibit different biases in strand polarity and proximity to terminal sequences in the insect host *Homalodisca vitripennis*. *Virology*, **442**, 12–19.